ARCHIVES OF ACOUSTICS
25, 2, 213–227 (2000)

PERIODIC CRACK-MODEL OF COMB TRANSDUCERS: EXCITATION OF INTERFACE WAVES

E. DANICKI

Polish Academy of Sciences
Institute of Fundamental Technological Research
(00-049 Warszawa, Świętokrzyska 21, Poland)
e-mail: edanicki@ippt.gov.p

A model for a comb transducer is proposed and analyzed. It is shown that interface waves are generated in the comb-sample contact area. The interface waves are leaky waves that transport acoustic energy along the interface towards the comb edges, where it is eventually converted into surface acoustic waves propagating outside the comb. By including piezoelectric effects in the comb and the sample materials, it is possible to analyze the incident bulk wave generated by embedded metal strips on both sides of the interface. Approximations for the scattered wavefield and the relationship describing the energy transfer along the interface are derived. Numerical examples are presented.

1. Introduction

Comb transducers may be used for the generation of finite-amplitude surface acoustic waves in solids [1]. For this purpose, where transducer efficiency is a crucial parameter, an optimization of the structure is badly needed; this requires transducer modelling.

There is not satisfactory theoretical model of combs in literature for this purpose. An existing model [10] exploits weak-coupling assumption between a comb and a sample. Even if this could be somehow realized experimentally allowing Rayleigh wave to propagate unperturbed under the comb, the efficiency of bulk to surface wave transformation would be weak because of strong incident wave reflection at almost stress-free comb-sample interface.

Here, a model is proposed that will help to determine the comb's main parameters as well as the main phenomena that transform an incident bulk wave into surface waves under the comb. It will be shown that this transformation is a by-product [2] of the wave scattering by periodic voids that form between the comb teeth and the sample surface, as shown in Fig. 1(a).

2. Description of the model

In the model illustrated in Fig. 1(b), the typically thin voids of the comb are replaced by cracks. To simplify analysis, periodic cracks are assumed with period Λ and width

$\Lambda - w$. Because the system is infinite, surface waves cannot propagate along a free surface. Instead, an interface wave [3] (a "crack wave") can exist at the cracked interface between the two solid halfspaces of the comb and the sample. These crack interface waves would be transformed into surface waves at the edges of a real finite comb. This phenomenon is not analyzed here, since we are interested primarily in the transformation phenomenon of the incident wavebeam into an interface wave during its scattering by periodic cracks. The system under consideration is two-dimensional, with infinite cracks in the z-direction and a wavefield independent of z.

The incident wavebeam is assumed to be finite. This makes it possible to evaluate the crack wave amplitude excited by the incident wavebeam at a position just outside the area of incidence. In a typical comb transducer, the incident wave is generated by a piezoelectric plate transducer placed on the top of comb; the generated wavebeam of roughly uniform amplitude propagates towards the comb-sample interface, as shown in Fig. 1(a). (Naturally, the wavebeam undergoes diffraction as it propagates, so that its exact shape at the comb-substrate interface may deviate from uniformity.)

In this model, the incident wave is generated using the piezoelectric effect. To do this, we include weak piezoelectricity in both of the elastic halfspaces (comb and sample), and embed periodic metal strips on either side of the interface (without disturbing the material mechanical integrity). These strips can be either grounded or connected to an external voltage source in the manner of an ordinary piezoelectric transducer electrode. The other electrode is grounded to the fully metallized interface at $y = 0$, as shown in Fig. 1(b). The strips excite bulk waves in the same way that an ordinary piezoelectric transducer does. Current is also induced in the grounded strips by the local wavefield in the same way as in piezoelectric transducers. This effect will be later exploited to detect the amplitude of the scattered wavefield at a given strip position in either of two halfspaces.

The strips are periodic with the same period Λ as the cracks, but have a fairly wide width w_e. Therefore, applying a voltage to a series of strips mimics a single wider transducer electrode and thus generates a wider wavebeam. The polarization of the wavebeam can be either longitudinal or shear, depending on the piezoelectricity of the solid halfspaces. Assuming that the y-axis is perpendicular to the interface and the strips, and that the x-axis lies along the periodic system of cracks and strips, the piezoelectric modulus e_{22} results in the generation of longitudinal normal propagating incident wavebeam, while e_{26} will generate a shear incident wavebeam. The wavenumbers of the longitudinal and shear waves are denoted by k_l and k_t, respectively. The grounded strip current will be correspondingly sensitive to either one or the other component of the local wavefield.

In summary, by including piezoelectricity in the comb and sample materials and by embedding periodic strips on either side of the the interface, we are able to 1) generate a normal incident wavebeam of the required width and polarization, and 2) detect the local wavefield on either side of the interface. We are most interested in the detection of the scattered wavefield amplitude at different positions along the periodic system of strips, that is, at different lateral distances from the incident wavebeam. Figure 1(c) presents

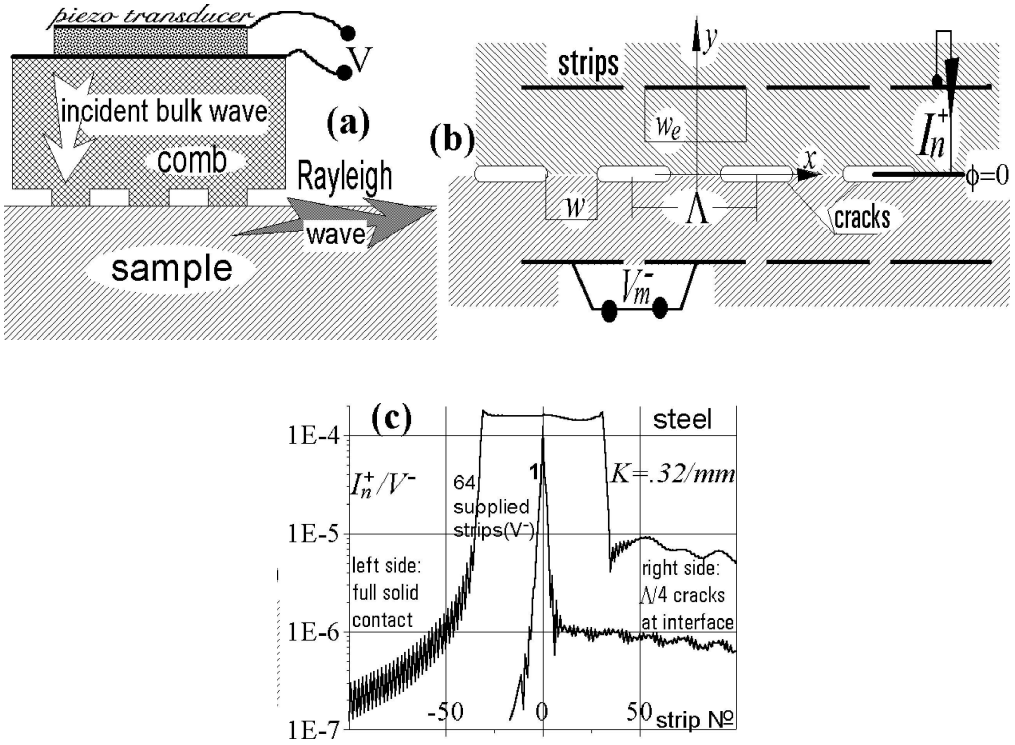

Fig. 1. a) Schematic diagram of a comb transducer with a plate piezoelectric transducer on top, attached to the sample surface. The period of the comb teeth is chosen equal to the wavelength of the generated surface wave. It is assumed that the voids formed between the comb teeth and the sample are thin. b) In the model, voids are modelled by periodic cracks at the interface of two elastic halfspaces (comb and sample). A side effect of this model is that the generated surface wave can propagate in both halfspaces as an entire interfacial wave. Moreover, the system is considered infinite. Mechanical contact between the cracks that model the tooth-sample contact can be either solid or sliding. Weak piezoelectricity of the halfspaces is included. The embedded wide ($\Delta_e = -0.9$) ideal conducting strips on both sides of the interface help to model the generation of a normal incident wavebeam of finite aperture width, and to detect the scattered wavefield in any lateral position with respect to the incident wave. c) Illustration of how the inclusion of piezoelectricity works. One or 64 strips in the lower strip system are supplied with voltage V^- and generate the normal incident wavebeam onto the interface. The currents I_n^+ induced in strips on the other side (which is grounded to the interface plane) depend on the strips' lateral position with respect to the incident beam (horizontal axis is the strip number). The current amplitude is shown in a logarithmic scale for two cases: with perfectly contacting halfspaces without cracks (left), and with relatively narrow cracks that do not allow interface waves to exist (right). In both cases, the plots represent typical transmission patterns with limited diffraction effects due to the small distance $2d$ between the embedded strips. The small values of I^+/V^- result from the weak piezoelectric effect assumed: $e_{26} = 1\,\mathrm{Cm}^{-2}$ for generation of a shear incident wave. In all of the figures, both the comb and sample are assumed to be made of steel with the following parameters: $k_t = 0.3097/\mathrm{mm}$, $k_l = 0.1695/\mathrm{mm}$, and $\rho = 7700\mathrm{kg\,m}^{-3}$ (at $\omega = 10^6\,\mathrm{s}^{-1}$).

examples of how the system works for solid contact between the halfspaces (without cracks), and for certain system of narrow cracks between the halfspaces that does not allow interface waves to propagate. Under these conditions, the figure presents typical diffraction patterns plotted on a log scale; it will be later compared to Fig. 2.

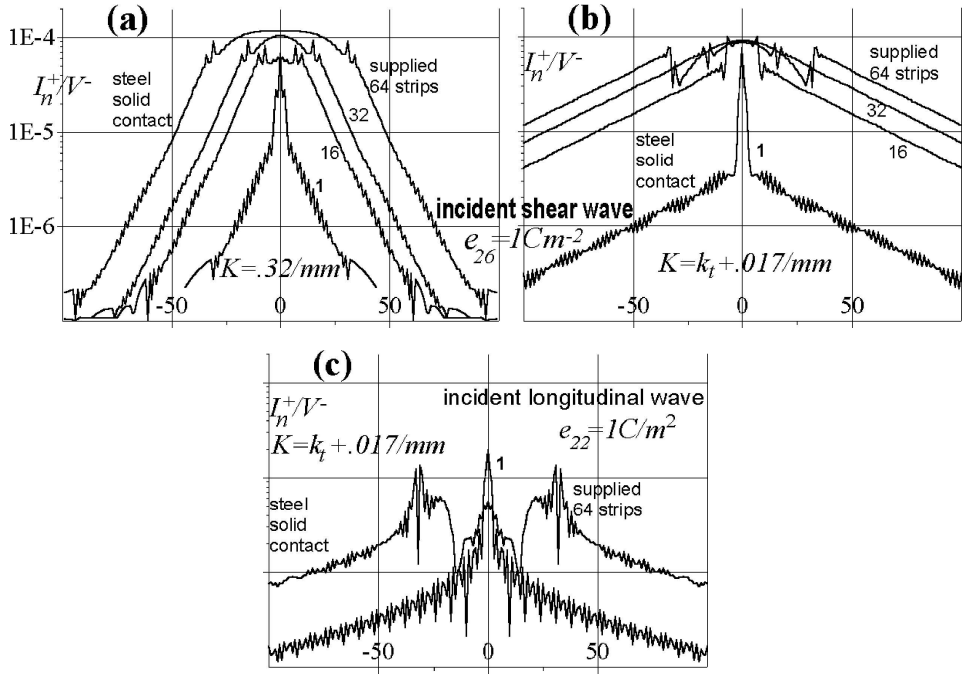

Fig. 2. a) Diffraction pattern for cracks of width $3/4\Lambda$ wide enough for interface waves to exist, for crack period $\Lambda = 2\pi/K$, for comparison with (b) plotted for another crack period. The strong dependence on K suggests a resonant phenomenon of the wave scattering. Three features are worth mentioning with respect to Fig. 1(c): 1) almost the same maximum signal level as for direct, unperturbed transmission by cracks; 2) much wider range of the scattered pattern; and 3) linear slope of the pattern when plotted logarithmically, which shows the exponential decaying phenomenon involved. These all confirm the following interpretation. The incident wavebeam is scattered by cracks and simultaneously an interface leaky wave is generated. This wave propagates along the interface delivering acoustic power to large distances from the area of incidence, and reradiates bulk waves due to a leakage phenomenon. The reradiated bulk waves are detected by strips much farther away from the incident wavebeam than would be possible with pure diffraction phenomenon only. The linear slope confirms that we are indeed dealing with a leaky interface wave, as opposed to scattering of a longitudinal wavebeam (e_{22} =1 Cm^{-2} applied instead of e_{26}) drawn in figure (c), that does not excite interface waves in this system. There is no long range of the scattered wavefield, and no linear slope of the pattern outside the area of incidence. (A small interface wave may still exist, however, which is excited by nonuniformities in the incident wave.)

3. Characterization of a layered halfspace

Introducing a potential ϕ of the electric field $E_i = -\phi_{,i}$, $i = 1, 2$, the wave-motion of a piezoelectric body is governed by the following system of equations:

$$\begin{aligned} T_{ij} &= c_{ijkl}u_{k,l} + e_{lij}\phi_{,l}\,, \\ D_i &= e_{ijk}u_{j,k} - \epsilon_{ij}\phi_{i,j}\,, \\ \rho u_{i,tt} &= T_{ij,j}\,, \\ D_{i,i} &= 0, \end{aligned} \tag{1}$$

where T is the stress, D is the electric induction, u is the displacement, c is the stiffness tensor of an assumed isotropic body with Lamé constants λ and μ, and ρ is the mass

density. e and ϵ are the piezoelectric and dielectric constants. Here, only $e_{222} = e_{22}$ in matrix notation or $e_{212} = e_{26}$ may be assumed different from zero and equal 1 Cm^{-2}, and ϵ_{ii}/ϵ_0 is set to 10.

In this paper, a time-harmonic field $\exp(j\omega t)$ is considered, so that $\rho u_{i,tt} = -\rho\omega^2 u_i$. Later, if a spatial-harmonic field $\exp(-jpx - jsy)$ is considered, Eqs. (1) can be transformed into Stroh equation [4]

$$\mathbf{H}\,\mathbf{F} = q\,\mathbf{F}, \tag{2}$$

where an eigenvalue $q = s/p$ characterizes the mode dispersion property, in which the polarization is described by an eigenvector $\mathbf{F} = [jpu_i, jp\phi, T_{2l}, D_2]^T$, $i, l = 1, 2$. The matrix $\mathbf{H}$ depends on the material constants and on $\rho\omega^2/p^2$. $\mathbf{H}$ is a 6×6 matrix, because we neglect the wave-field dependence on z, as well as z-polarized transverse waves. The matrix is real for real p.

Solving Eq. (2) for a given spectral variable p, one obtains the eigenvalues q_n and wavevector components (p, s_n) of six possible modes $\mathbf{F}^{(n)}$, $n = 1, ..., 6$. Three of the modes ($n = 1, 2, 3$) satisfy the radiation conditions at $y \to \infty$ (the modes either carrying energy into infinity or decaying at $y \to \infty$), and the other three satisfy the corresponding radiation conditions at $y \to -\infty$. These two families of solutions to Eq. (2) will be exploited in constructing the solutions to the wavefields in the elastic halfspaces $y > 0$ and $y < 0$.

In the layered halfspace $y > 0$, the stress T_{2i}^+ at $y = +0$ and the surface electric charge is D^+ at $y = d$ are both assumed to be known in the form of a harmonic distribution $\exp(-jpx)$ (neglecting harmonic dependence on time) with corresponding complex amplitudes (with notation held unchanged). The superscript "+" denotes the field in the halfspace $y > 0$. Thus the boundary conditions which must be satisfied by the y-dependent wavefields are

$$\begin{aligned}
T_{2i}(y=0) &= T_{2i}^+, \\
\phi(y=0) &= 0, \\
T_{2i}(y=d-0) &= T_{2i}(y=d+0), \\
u_i(y=d+0) &= u_i(y=d-0), \\
D_2(y=d+0) &- D_2(y=d-0) = D^+, \\
\phi(y=d-0) &= \phi(y=d+0) = \phi^+.
\end{aligned} \tag{3}$$

(The second equation makes the interface plane electrically grounded, and the third and fourth equations ensure mechanical integrity across the strips.)

We seek the solution for $u_i(y=+0) = u_i^+$ and $\phi(y=d) = \phi^+$ which also satisfies the radiation conditions at $y \to \infty$ ($s_n = pq_n$):

$$\begin{aligned}
y \in (0, d): &\quad \sum_{n=1}^{6} A_n\,\mathbf{F}^{(n)} e^{-js_n y}, \\
y > d: &\quad \sum_{n=1}^{3} B_n\,\mathbf{F}^{(n)} e^{-js_n y}.
\end{aligned} \tag{4}$$

Substituting the above expansion into Eqs. (3) and eliminating expansion constants, one obtains

$$\begin{bmatrix} jpu_i^+ \\ jp\phi^+ \end{bmatrix} = \mathbf{G}^+(p) \begin{bmatrix} T_{2j}^+ \\ D^+ \end{bmatrix}, \qquad i,j = 1,2, \tag{5}$$

where the 3×3 matrix $\mathbf{G}^+$ can be evaluated numerically for any given value of the spectral variable p.

Note [4] that for p much larger than the bulk cut-off wavenumber k_t, all q_n are complex. Furthermore, the wavefield generated by the applied T^+ at $y = 0$, or by D^+ at $y = d$, is highly localized at these two planes and thus contributes nothing to the wavefield on the other plane. In conclusion, the value of $G_{33}(p \to \infty)$ is the same as in an infinite body without a boundary at $y = 0$, while $G_{ij}(p \to \infty)$, $i,j = 1,2$ is the same as for an elastic halfspace without the plane of charge at $y = d$. Moreover, the influence between these two planes vanishes at large p,

$$\mathbf{G}^+(p \to \infty) = \begin{bmatrix} G_{ij}(\infty) & 0 \\ 0 & G_{33}(\infty) \end{bmatrix}, \qquad i,j = 1,2. \tag{6}$$

In fact, $\mathbf{G}^+(p) \approx \mathbf{G}^+(\infty)$ for $p > p_\infty$, with p_∞ several times larger than k_t. This will help to solve the boundary-value problem formulated in the following section. Also note that $\mathbf{G}^+(-\infty) = -\mathbf{G}^+(\infty)$.

The matrix $\mathbf{G}^-(p)$ which describes the relation between $[jpu_i^-, jp\phi^-]^T$ and $[T_{2j}^-, D^-]$ of the halfspace $y < 0$ (with electric charge at $y = -d$) has similar properties. These two matrices, $\mathbf{G}^\pm$, are the planar harmonic Green's functions of the spectral variable p. They sufficiently characterize the comb ($y > 0$) and the sample ($y < 0$) halfspaces, with weak piezoelectricity. This relationship will be exploited below in the solution of the boundary-value problem for periodic cracks at the interface between these two halfspaces, and strips embedded at distance d on both sides of the interface $y = 0$.

4. Periodic boundary-value problem

We now formulate the above boundary-value problem for arbitrary p. Let us first note that $jp\phi$ is a Fourier transform of $E_1 = -\partial\phi/\partial x$. Similarly, jpu_i corresponds to the spatial function $U_i = -\partial u_i/\partial x$. For convenience, the boundary problem is formulated using the above x-derivatives instead of the functions themself, in the equations governing the body (Eq. (5)) as well as in the boundary conditions at the plane of strips ($y = \pm d$) and the plane of cracks ($y = 0$):

$$\left.\begin{aligned} E_1^\pm &= 0 \quad \text{on strips,} \quad x \in (-w_e, w_e) \\ D^\pm &= 0 \quad \text{between strips,} \quad x \in (w_e, \Lambda - w_e) \end{aligned}\right\} \; y = \pm d,$$

$$\left.\begin{aligned} T_{2i}^- = T_{2i}^+ &= 0 \quad \text{on cracks,} \quad x \in (w, \Lambda - w) \\ T_{2i}^- = T_{2i}^+ &= T_{2i} \quad \text{between cracks,} \quad x \in (-w, w) \\ U_i^+ &= U_i^- \quad \text{between cracks,} \quad x \in (-w, w) \end{aligned}\right\} \; y = 0, \tag{7}$$

for x in one periodic domain. The above equations concern the solid contact between the two halfspaces at the interface $y = 0$. Other simple boundary conditions exist for sliding contact, where $T_{21} = 0$, $x \in (-\Lambda/2, \Lambda/2)$, and the displacement continuity is $U_2^+ = U_2^-$ instead of $U_i^+ = U_i^-, i = 1, 2$ above. (Another simple, albeit nonphysical, case would be $T_{22} = 0$ at the interface and $U_1^+ - U_1^-$ between cracks.)

The first and the last equations in Eqs. (7), stated for the x-derivatives of the corresponding wavefields, do not sufficiently describe the boundary conditions at the strips and cracks. (A possible constant difference between u_i^+ and u_i^- makes it underdetermined.) The boundary conditions must be appended by conditions for the wavefield evaluated at a single point anywhere in the corresponding domain. These are called the "single-point" conditions, and here the point of $x = 0$ at the center of a strip or a comb tooth is used:

$$\begin{aligned} \int (U_i^+ - U_i^-)\, dx &= \overline{U}_i, \\ -\int E_1^{\pm}\, dx &= V^{\pm}. \end{aligned} \tag{8}$$

$\overline{U}_i$ and $V_i^{\pm}$ are assumed to be known. $V^{\pm}$ are the strip potentials, and $\overline{U}_i = 0$ ensures the perfect contact of both halfspaces between cracks. Otherwise, the comb teeth would be separated by a constant distance $\overline{U}_i$.

We now introduce a relationship between $U_i = U_i^+ - U_i^-$, T_{2i}, $D^{\pm}$ and $jp\phi^{\pm}$ in the spectral domain that results from Eq. (5), accounting for $\mathbf{T} = \mathbf{T}^+ = \mathbf{T}^-$ for any x at the interface $y = 0$ $(i, j = 1, 2)$:

$$\begin{gathered} \begin{bmatrix} \mathbf{U} \\ \mathbf{E} \end{bmatrix} = \mathbf{g} \begin{bmatrix} \mathbf{T} \\ \mathbf{D} \end{bmatrix}, \\ \mathbf{g} = \begin{bmatrix} G_{ij}^+ - G_{ij}^- & G_{i3}^+ & -G_{i3}^- \\ G_{3i}^+ & G_{33}^+ & 0 \\ G_{3i}^- & 0 & G_{33}^- \end{bmatrix}, \qquad \mathbf{g}_\infty = \begin{bmatrix} \overline{\mathbf{g}}_\infty & \mathbf{O} \\ \mathbf{O} & \tilde{\mathbf{g}}_\infty \end{bmatrix}, \end{gathered} \tag{9}$$

where $i, j = 1, 2$. In our notation, $\mathbf{E} = [E_1^+, E_1^-]^T$, $\mathbf{D} = [D^+, D^-]^T$, $\mathbf{U} = [U_i]$, $\mathbf{T} = [T_{i2}]$, and $\mathbf{O}$ is a zero matrix. The matrix $\mathbf{g}$, which depends on p, assumes the limit $\mathbf{g}_\infty$ at $p \to \infty$. Under certain approximations and for properly chosen, sufficiently large p_∞, we may use $\mathbf{g}(p > p_\infty) = \mathbf{g}_\infty$. Note that $\mathbf{g}(-p_\infty) = -\mathbf{g}(p_\infty)$.

For completeness, an average measure of the wavefield on the strips and between the cracks (that is, on the comb teeth), can be defined as follows:

$$\begin{aligned} \overline{\mathbf{T}} &= \int_{-\Lambda/2}^{\Lambda/2} \mathbf{T}\, dx, \quad \text{where } \mathbf{T} = [T_{i2}^+], \\ \mathbf{I} &= [I^+, I^-]^T = j\omega \int_{-\Lambda/2}^{\Lambda/2} \mathbf{D}\, dx. \end{aligned} \tag{10}$$

The integrations are originally taken over a comb tooth between neighboring cracks or over a strip and then extended into the full period Λ accounting for Eqs. (7).

5. A method of solution

We now apply the method used in an earlier paper [3] with an extension concerning the electric field [5]. This method is presented here only briefly. First, the wavefield is expanded into a Bloch series (summation over n) with its expansion coefficients represented in the so-called BIS expansion [5]

$$\begin{aligned}
\mathbf{T} &= \sum_{n=-\infty}^{\infty} \sum_{m} \mathbf{T}^{(m)} P_{n-m}(\Delta) e^{-j(r+nK)x}, \\
\mathbf{U} &= \sum_{n=-\infty}^{\infty} \sum_{m} \mathbf{U}^{(m)} S_{n-m} P_{n-m}(\Delta) e^{-j(r+nK)x}, \\
\mathbf{D} &= \sum_{n=-\infty}^{\infty} \sum_{m} \mathbf{D}^{(m)} P_{n-m}(\Delta_e) e^{-j(r+nK)x}, \\
\mathbf{E} &= \sum_{n=-\infty}^{\infty} \sum_{m} \mathbf{E}^{(m)} S_{n-m} P_{n-m}(\Delta_e) e^{-j(r+nK)x},
\end{aligned} \tag{11}$$

where $\Delta = \cos Kw$, $\Delta_e = \cos Kw_e$, $S_\nu = 1$ for $\nu \geq 0$ or -1 otherwise, and P_ν is the Legendre function. These expansions satisfy the boundary conditions (7) for any expansion coefficients marked by the superscript "(m)".

The summation over m has finite limits $[-M, M+1]$ depending on K, k_t, and d. These limits are set following the general rule that, for certain large $|n| > M$, the system of equations (13) that results should be satisfied automatically for arbitrary $\mathbf{T}^{(0)}$ and $\mathbf{D}^{(0)}$ (within an accepted accuracy [3, 6]). In computations with $K \approx k_t$ and $d \approx \Lambda/2$, we have found that $M = 3$ is satisfactory. In the above expansions, r is limited to one Brillouin zone $r \in (0, K)$; note that all wavefield amplitudes involved in the above equations depend on this reduced spectral variable.

Accounting for the property of $\mathbf{g}_\infty$, we notice that [6]

$$\begin{aligned}
\mathbf{U}^{(m)} &= \overline{\mathbf{g}}_\infty \mathbf{T}^{(m)}, \\
\mathbf{E}^{(m)} &= \tilde{\mathbf{g}}_\infty \mathbf{D}^{(m)}.
\end{aligned} \tag{12}$$

Substitution of expansions (11) into Eq. (9) yields for any n

$$\sum_{m} \left[\mathbf{g}_\infty S_{n-m} - \mathbf{g}(r+nK) \right] \begin{bmatrix} \mathbf{T}^{(m)} P_{n-m}(\Delta) \\ \mathbf{D}^{(m)} P_{n-m}(\Delta_e) \end{bmatrix} = 0. \tag{13}$$

This is satisfied automatically for $|n| > M$ provided that M is chosen properly ($M > k_t/K$).

Let us now discuss the first equation of the system (13) concerning the mechanical field $\mathbf{T}$ and $\mathbf{U}$ at the interface. If the systems of strips are embedded deeply inside the halfspace (large d), then $G_{i3}^{\pm}$ have significant nonzero values only for such $p = r + nK$ for which the eigenvalues q are real. (Otherwise, the exponential functions in Eq. (4) vanish, preventing any significant influence of the electric charge on the wavefield at the

interface.) A real eigenvalue q_l corresponds to a propagating mode $\mathbf{F}^{(l)}$ excited by the strips which is an incident bulk wave onto the crack system. We are interested primarily in normal incidence for which $p \approx 0$ and (if K is not too small) $r \approx 0$. Accounting for the zeros $\mathbf{O}$ in the matrix $\mathbf{g}_\infty$ of Eq. (9), the incident wave is represented by the right hand side of

$$\sum_m \left[\overline{\mathbf{g}}_\infty S_{n-m} - \overline{\mathbf{g}}(r+nK)\right] \mathbf{T}^{(m)} P_{n-m}(\Delta) = \delta_{n0}\tilde{\mathbf{U}}, \tag{14}$$

where δ_{ij} is a Kroenecker delta. $\tilde{\mathbf{U}} = [G^+_{i3}(r+nK), -G^-_{i3}(r+nK)]\mathbf{D}_n$ where $\mathbf{D}_n$ is the n-th harmonic component of Bloch series (11) and depends indirectly on the voltage applied to the metal strips. It follows from Eq. (5) that $\tilde{\mathbf{U}} = jr[\tilde{u}^+_i(r+nK) - \tilde{u}^-_i(r+nK)]$ can be considered known, because for weak piezoelectricity $\mathbf{D}_n$ can be evaluated directly from the known strip potentials [5, 6], neglecting the mechanical field. Thus $\tilde{u}^\pm_i(r+nK)$ are particle displacements associated with the incident waves generated by either the upper or lower system of strips.

The nontrivial equations in Eq. (13) are those for $-M \le n \le M$. To close the system of equations, we need to account for Eqs. (8), which are

$$\begin{aligned} \sum_m (-1)^m \mathbf{U}^{(m)} P_{-m-r/K}(-\Delta) &= \frac{K}{\pi}\overline{\mathbf{U}} \sin \pi r/K, \\ \sum_m (-1)^m \mathbf{E}^{(m)} P_{-m-r/K}(-\Delta_e) &= \frac{K}{\pi}\mathbf{V} \sin \pi r/K, \end{aligned} \tag{15}$$

where $\mathbf{V} = [V^+, V^-]^T, \overline{\mathbf{U}} = [\overline{U}_i]$. Equations (13) and (15), accounting for (12), allow us to evaluate all of the expansion coefficients in Eqs. (11) and their dependence on $\overline{\mathbf{U}}$ and $\mathbf{V}$.

Finally, substitution of the expansion (11) into Eqs. (10) results in

$$\begin{aligned} \overline{\mathbf{T}} &= \Lambda \sum_m \mathbf{T}^{(m)} P_{-m-r/K}(\Delta), \\ \mathbf{I} &= j\omega\Lambda \sum_m \mathbf{D}^{(m)} P_{-m-r/K}(\Delta_e). \end{aligned} \tag{16}$$

Accounting for Eqs. (15), we obtain

$$\left[\overline{\mathbf{T}}, \mathbf{I}\right]^T = \overline{\mathbf{Y}}(r) \left[\dot{\mathbf{U}}, \mathbf{V}\right]^T \sin \pi r/K. \tag{17}$$

For further convenience, we have introduced the notation $\dot{\mathbf{U}} = j\omega[\overline{U}^+_i - \overline{U}^-_i]$ which has the physical meaning of the comb tooth velocity relative to the sample, Eq. (8) (Fig. 3). Note that the above solution depends on r, a reduced spectral variable whose value is in the domain of one Brillouin zone $(0, K)$: $\overline{\mathbf{Y}}(K-r) = \overline{\mathbf{Y}}(r)$. This results from the symmetry concerning the mode propagation direction. $\dot{\mathbf{U}}$ and $\mathbf{V}$ may also be functions of r in this domain without any change in the above considerations.

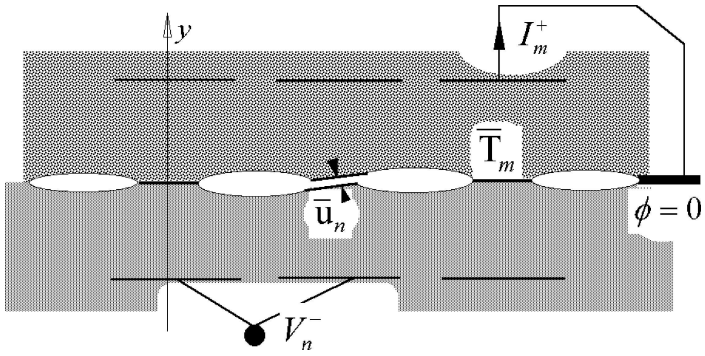

Fig. 3. An interpretation of the transfer relationship, Eq. (19), and the quantities involved. $I_m^{\pm}$ is the current in strip number m excited by the local wavefield at the strip position $x = m\Lambda$, above or below the interface (marked by superscript $\pm$). This wavefield results from the incident wavebeam generated by strip number n to which a voltage $V_n^{\pm}$ is applied relative to the grounded interface $y = 0$; the other strips are grounded. The local wavefield can be also characterized by a force $\overline{\mathbf{T}}_m$ that the comb tooth of number m exerts on the sample surface. An artificial comb tooth displacement $\overline{\mathbf{u}}_n$ with respect to the sample surface may be used to represent the incident wavebeam local amplitude. (This is a quantity that can be evaluated from the known amplitude of incident wavebeam at a given comb tooth.) Note that we may apply only the difference $\overline{u}_i^+ - \overline{u}_i^-$ which is constant over an entire comb tooth (contact area between cracks). The position and the inclination of this area with respect of the interface plane $y = 0$ results from the solution. It is marked in the figure by two parallel bounds of lower and upper halfspaces between cracks, which are somewhat shifted and inclined with respect to $y = 0$ plane.

6. Discrete functions

In fact, $\mathbf{V}$ and $\overline{\mathbf{U}}$ are the Fourier transforms of discrete functions which depend on the strip or crack number l along their periodic positions in the systems. In particular, for known strip potentials $\mathbf{v}(l) = [V^+(l), V^-(l)]^T$ and comb tooth displacements with respect to the sample surface $\overline{\mathbf{u}}(l) = [u_i^+ - u_i^-]$ with velocity $\dot{\mathbf{u}} = j\omega\overline{\mathbf{u}}$, the inverse discrete Fourier transforms [7] are defined by

$$\begin{aligned} \mathbf{v}(k) &= K^{-1} \int_0^K \mathbf{V}(r) e^{-jrk\Lambda}\, dr, \\ \dot{\mathbf{u}}(k) &= K^{-1} \int_0^K \dot{\mathbf{U}}(r) e^{-jrk\Lambda}\, dr. \end{aligned} \tag{18}$$

It is evident that $\mathbf{V}(r)$ must be equal to the sum over all strips, $\sum_l \mathbf{v}(l) \exp(jrl\Lambda)$, and similarly $\dot{\mathbf{U}}(r) = \sum_k \dot{\mathbf{u}}(l) \exp(jrl\Lambda)$.

Substitution of the above into Eqs. (17) yields the discrete spatial dependence

$$\begin{aligned} \begin{bmatrix} \overline{\mathbf{T}}(k) \\ \mathbf{I}(k) \end{bmatrix} &= \mathbf{Y}(k-l) \begin{bmatrix} \dot{\mathbf{u}}(l) \\ \mathbf{v}(l) \end{bmatrix}, \\ \mathbf{Y}(m) &= K^{-1} \int_0^K \overline{\mathbf{Y}}(r) e^{-jrm\Lambda} \sin \pi r/K\, dr. \end{aligned} \tag{19}$$

The integrand $\overline{\mathbf{Y}}(r)$ is a regular function, so the evaluation of the above integral can be easily performed using the convenient FFT algorithm.

This relationship has the following interpretation for the natural case of $\dot{\mathbf{u}}(l) = 0$ for all l (Fig. 3). Assume that only one, zeroth strip in the lower system of strips has an applied voltage $v^-(l=0) = v^-_{l=0}$ (using alternative subscript numbering). It results from Eq. (19) that the currents of this and neighboring strips in this lower, $I^-(k) = I^-_k$, and upper, I^+_k systems of strips are excited in spite of the metallized grounded screening interface $y = 0$. This can only be caused by means of a bulk wavebeam transmitted through the interface, that was excited by the strip. Currents are excited in strips positioned a lateral distance $|l-k|\Lambda$ from the wavebeam.

Figure 1(c) presents the excited currents I^+_k in an example where there are no cracks at the interface (perfect contact between halfspaces), or weakly scattering cracks. It represents simple wavebeam transmission through a small distance $2d$ so that the diffraction effect is small, resulting in almost uniform detected wavebeam. The range $|k-l|\Lambda$ of the detected field is confined to the excited wavebeam width (1 or 64 strip periods in the figure).

In the case of strongly scattering cracks, for instance for wider cracks at the interface as in Fig. 2, the scattered field propagates in all directions and can be detected over a much wider range (that is, by strips of numbers k much different from those with number l to which voltage has been applied). Another phenomenon that causes an excessively wide range of the scattered field will be discussed below.

Equations (19) yields yet another wavefield characteristic, the force $\overline{\mathbf{T}}(k)$ at the interface. Following its definition (10), this is a vector of the full force between two neighboring cracks. Within the model framework of a comb transducer, it corresponds to the total force exerted by a single comb tooth of number k on the sample surface. This force represents the local wavefield at the interface and, when evaluated for different k, similar figures can be obtained as discussed above for strip currents. Finally, we note that the assumption of weak piezoelectricity makes the wave scattering by strips negligible.

7. The scattered field approximation

It was shown in an earlier paper [3] that there can be leaky interfacial waves guided along the system of cracks. They are attenuated and have complex wavenumber $k_c = K - r_c$ close to k_t for cracks embedded in otherwise homogeneous media. It has also been shown that such waves can be excited by a bulk wave at close to normal incidence, for certain crack wavenumbers K within a narrow range just above k_t. Above, we developed a suitable tool for analysis these phenomena, and indeed, they appear in the scattering pattern presented in Figs. 2(a) and (b).

The first striking feature of these plots on a log scale is a linear slope of the wavefield amplitude outside the domain of incidence. This means that the scattered field decays exponentially in the area where there are no propagating incident or reflected wavebeams. Such exponential decay is characteristic of interfacial waves $\exp(-jr_c x)$. The discussed figures must thus present leaky interface waves existing outside the area of incidence.

In the context of this theory, a guided mode in the system is represented by a pole of the integrand of Eq. (19) at $r = r_c$, and the excited amplitude of the mode can be evaluated as a residuum of this integral evaluated on the complex plane r.

Here we propose the following approximation to $\overline{\mathbf{Y}}(r)$ at $r \approx r_c \approx 0$ in the case of close to normal incidence:

$$\overline{\mathbf{Y}}(r) = \text{const} + \left\{ \frac{1}{r - r_c} + \frac{1}{(K - r) - r_c} \right\} \mathbf{a} - \left\{ \frac{1}{r + r_c} + \frac{1}{(K - r) + r_c} \right\} \mathbf{a}. \tag{20}$$

The particular form of the above approximation results from the system periodicity, the symmetry with respect to the propagation direction, and the fact that r is the reduced spectral variable with values in one Brillouin zone only, $(0, K)$. The approximation coefficients can be easily found numerically. For instance, r_c is a zero of $1/\overline{Y}_{nn}$ (the matrix diagonal element).

The integration path (19) of the approximated terms is first extended to infinity, then closed in the lower or upper complex halfspaces where the integrands satisfy the Jordan lemma [6]. The residua yield the interfacial components of the scattered wavefield, while the regular parts of integrands contribute only to the localized wavefield within or near the domain of incidence. Example results are plotted in Fig. 4. Here, directly evaluated wavefields from Eq. (19) are presented on the left half of the figure for comparison with the approximated wavefields from Eq. (20) plotted in the right half, for two different

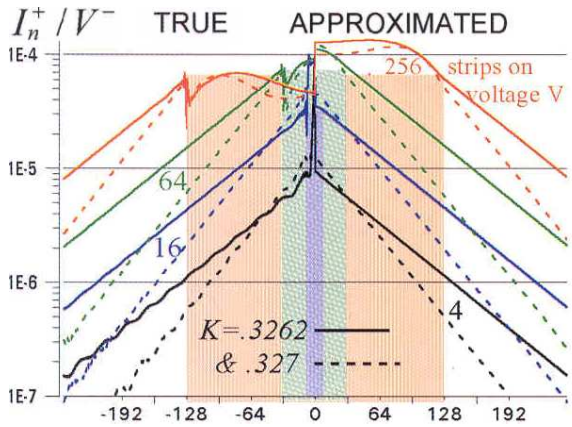

Fig. 4. Comparison of an approximated diffraction pattern form Eq. (20) (right) to that evaluated directly from Eq. (19) (left), for various values of K. The transverse incident wave ($e_{26} \neq 0$) and crack width are like those in Fig. 2. The area of incidence is denoted by the shadowed region. The most important wavefield amplitude is that at the edge of incidence, which corresponds to the edge of comb. The field of this amplitude is eventually converted into the surface wave outside the comb. A large range of incident wavebeam aperture widths is presented to show that this edge amplitude value can be obtained with a relatively small incident beamwidth. The fact that the amplitude cannot be made larger by applying a wider wavebeam is reasonable: the excited interface wave displacement amplitude cannot exceed the corresponding amplitude of the incident wave. The most important result presented in this figure is an excellent agreement between the approximated and numerically-evaluated scattering patterns, confirming 1) the validity of the approximation, which makes calculations much easier, and 2) the resonant phenomenon of the analyzed scattering. Indeed, the approximation is based on a singular function in spatial frequency like the singular function of time frequency that describes a typical resonant circuits.

crack wavenumbers K and different aperture widths of the incident wavebeams. Note the quality of the approximation outside the incidence domain. The approximation does not include any directly transmitted or reflected bulk waves and thus is inappropriate for the domain of incidence.

This allows us to make a final interpretation of the examples presented in Figs. 2 and 4. Interface crack waves are excited in the incidence area of a finite wavebeam onto the cracks and propagate at the interface along the crack systems, leaking energy into bulk waves. This wave is detected by strips much farther away from the incident wavebeam. The leakage is caused by the 0-th order Bloch component that is a propagating mode of wavenumber $-r_c = k_c - K$, close to zero. It represents an almost normal outgoing bulk wave that takes away energy from the crack wave, making it leaky and weakly decaying on its propagation path. The further away, the weaker the reradiated bulk wave and the current induced in strips. This exponential decaying yields a linear slope of the scattering pattern plotted in a log scale in the figures.

Two features of Fig. 4 are worth mentioning here. First, the amplitude of the excited interface waves is never greater than a certain limit, even for wider incident wavebeams (corresponding to larger number of teeth in a comb). Second, this maximum amplitude takes place at the edge of the domain of incidence (that is, at the comb edge). In a real, finite comb, the excited interfacial waves will transform into surface waves at the edge of comb (at the boundary between the edge of the transducer and the free undisturbed surface of a sample). Thus from an application point of view, a comb with only the minimum number of teeth to yield the maximum crack wave amplitude at the edge of incident wavebeam is needed.

8. The interface wave-field

Equations (19) also suggests the possibility of analyzing interface waves in the system by applying $\dot{\mathbf{u}}_l$ instead of $\mathbf{v}_l$. It follows from Eq. (14) that this may be an indirect way of accounting for the incident wavebeam generated by the strips. Here, we discuss its physical significance.

In the analysis that follows, a close to normal incidence is assumed: $r \approx 0$ and $K > k_t$, which in particular means that only the 0-th order Bloch component represents propagating modes in the system. There are no other propagating modes, nor is there longitudinal-transverse mode conversion during scattering.

Let us start with Eq. (14) taken at $n = 0$ that involves the 0-th order Bloch components of incident, transmitted and reflected waves. Note that both $\overline{\mathbf{g}}(r)$ and $\tilde{\mathbf{U}}$ are proportional to r, Eqs. (5) and (9). Thus for small r and accounting for the physically correct condition that $\overline{\mathbf{U}} = 0$, we may rewrite Eqs. (14) for $n = 0$ and the first of Eqs. (15) in form

$$\begin{aligned} \sum_m S_{-m}\mathbf{U}^{(m)}P_{-m}(\Delta) &= \sum_m \overline{\mathbf{g}}(r)\mathbf{T}^{(m)}P_{-m}(\Delta) + \tilde{\mathbf{U}}, \\ \frac{1}{r}\sum_m \Big[S_{-m}\mathbf{U}^{(m)}P_{-m}(\Delta) - \frac{r}{K}(-1)^m p_{-m}(-\Delta)\overline{\mathbf{g}}_\infty \mathbf{T}^{(m)}\Big] &= \overline{\mathbf{U}} = 0, \end{aligned} \tag{21}$$

where $p_k(\cdot) = \partial_\nu P_{k+\nu}(\cdot)|_{\nu=0}$ and $P_n(-\Delta) = S_n(-1)^n P_n(\Delta)$. Accounting for the finite terms only at $r \to 0$, we obtain

$$\begin{aligned} \sum_m S_{-m}\mathbf{U}^{(m)}P_{-m}(\Delta) &= 0, \\ \sum_m \left[\{\overline{\mathbf{g}}(r)/r\}_{r\to 0}P_{-m}(\Delta) - (-1)^m \frac{p_{-m}(-\Delta)}{K}\overline{\mathbf{g}}_\infty\right]\mathbf{T}^{(m)} &= -\{\tilde{\mathbf{U}}/r\}_{r\to 0}. \end{aligned} \tag{22}$$

It results from the last equation that $\overline{\mathbf{U}} = -\{\tilde{\mathbf{U}}/r\}_{r\to 0}$ is an equivalent quantity that can be applied in Eq. (15) to describe the incident wave at the interface.

In summary, for close to normal shear (t) or longitudinal (l) incident waves, we can evaluate $\dot{\mathbf{U}} = j\omega\overline{\mathbf{U}}$ which appears in Eq. (17) to describe the incident wavebeam in equivalent manner. For example, for a uniform incident wavebeam, $\dot{\mathbf{u}}_l$ involved in Eq. (19) is constant within a limited range of l depending on the wavebeam aperture width. This greatly simplifies the model of comb transducers, because we no longer need to include in the model the piezoelectric plate transducer on the top of comb. We need use only a quarter of Eqs. (19), only that for $\overline{\mathbf{T}}_k$ and $\dot{\mathbf{u}}_l$ in which $\dot{\mathbf{u}}_l$ describes the incident wave at a given comb tooth of number l (assumed uniform over an entire tooth, Fig. 3). $\overline{\mathbf{T}}_k$ is the resulting force exerted by the comb tooth of number k on the sample surface. In the applied notation, $-\mathrm{Re}\{\sum_l \overline{\mathbf{T}}_l\dot{\mathbf{u}}_l^*\}/2$ is the delivered power by the incident wavebeam.

9. Conclusions

In this paper, we have analyzed a somewhat elaborate system to show that resonant generation of interface waves takes place when a bulk wave at close to normal incidence is scattered by periodic cracks with certain parameters. The phenomenon was shown to be governed by a transfer function $\mathbf{Y}$ whose spectral form has a pole in a wavenumber domain (also called the spatial frequency domain). This is analogous to a pole in the frequency domain of an ordinary resonant electric circuit. The phenomenon it describes is the resonance in the spatial domain, with a periodic force caused by periodic contact between the comb and the sample halfspaces.

The spatial transfer function $\mathbf{Y}(m)$, Eq. (19), yields a powerful tool for analysis of variety of comb transducers. It can be directly applied, for instance, in analysis of a "special comb" proposed recently [11], where each comb teeth are excited with different phases, like in the case of obligue incidence of bulk wave onto the comb-sample interface. This encourages us to develop the introduced and presented here approach into a full comb transducer model.

Numerical examples have been presented for cracks embedded in otherwise homogeneous media. However, similar results can be obtained within the presented general theory for cracks at the interface of two different solid halfspaces, with solid or sliding contact between cracks. These results fully confirm the main thesis of this and a previous paper [3] about the resonant scattering of close to normal incident waves by cracks. Yet another generalization of the presented theory can be made by applying it to a multi-periodic system of cracks: they will look like periodic combs separated by some distance,

each one with several teeth [8]. Another generalization is for oblique incidence, which is a 3-dimensional problem [9].

Future plans include applying this theory to the detailed investigation of comb transducers, for instance the frequency and time responses of the comb, the optimization of comb material for a given sample material, the number of teeth, and so forth.

Acknowledgements

Financial support was provided by the Polish-US Maria Skłodowska Curie Joint Fund II under Grant No. PAN/NIST-97-300. The author gratefully acknowledges helpful discussion with Dr. Donna C. Hurley at the National Institute of Standards and Technology and kind assistance in the preparation of this manuscript during her visit in the Institute of Fundamental Technological Problems earlier this year. This paper was originally submitted to The Journal of the Acoustical Society of America in April 1999 (and withdrawn in May 2000 because of unbearable slow peer-review process giving no chance of publication before the end on the above mentioned Grant). There are special thanks to its Associate Editor Prof. Dale Chimenti and to anonymous reviewers for comments concerning relevant literature that improved the text: the second paragraphs of Introduction and of Conclusions, and corresponding references result from these comments. (The last reference appeared after the paper submission; the peer-review delay made it possible to include this reference.)

References

[1] D.C. Hurley, *Nonlinear propagation of narrowband Rayleigh waves excited by a comb transducer*, J. Acoust. Soc. Am. (in press).

[2] E.J. Danicki and D.C. Hurley, *Resonant scattering phenomenon by in-plane periodic cracks*, J. Acoust. Soc. Am., **105**, 1225 (1999), CD-ROM: Collected Papers "Berlin 99", ISBN 3-9804568-5-4.

[3] E.J. Danicki *Resonant phenomena in bulk-wave scattering by in-plane periodic cracks*, J. Acoust. Soc. Am., **105**, 84–92 (1999).

[4] E.J. Danicki, *An approximation to the planar harmonic Green's function at branch points in wave-number domain*, J. Acoust. Soc. Am., **104**, 651–663 (1998).

[5] K. Bløtekjær, K.A. Ingebrigtsen and H. Skeie, *A method for analyzing waves in structures consisting of metal strips on dispersive media*, IEEE Trans. Electron Devices, **20**, 1133–1138 (1973).

[6] E. Danicki, *Excitation, waveguiding and scattering of EM and elastic waves by a system of in-plane strips or cracks*, Arch. Mech., **46**, 123–149 (1994).

[7] E.I. Jury, *Theory and application of the $\mathcal{Z}$-transform method*, Wiley, New York 1964.

[8] E. Danicki, *Spatial spectrum of electric charge on planar array of metal strips*, Electr. Lett., **31**, 2220–2221 (1995).

[9] E. Danicki, *Bending of a layered isotropic plate with periodic disbondings*, ASME J. Appl. Mech., **61**, 612–617 (1994).

[10] J.L. Rose, S.P. Pelts and M.J. Quarry, *A comb transducer model for guided wave NDE*, Ultrasonics, **36**, 163–169 (1998).

[11] J.L. Rose and S.P. Pelts, *A comb transducer model for guided wave mode control*, Review of Progress in Quantitative Nondestructive Evaluation, **18**, 1029–1037 (1999).